Geophysical Research Letters

RESEARCH LETTER
10.1029/2019GL083090

Key Points:
- Ocean model and reanalysis data sets show large spread, and no robust trend of the MC transport is found over the past decades
- Uncertainties in surface wind data are the primary cause for the large spread, and the NBL acts to attenuate the MC transport change
- The MC can be dramatically enhanced by westerly winds in the western Pacific through spinning up the cyclonic local recirculation

Supporting Information:
- Supporting Information S1

Correspondence to:
Y. Li,
liyuanlong@qdio.ac.cn

Citation:
Duan, J., Li, Y., Wang, F., & Chen, Z. (2019). Multidecadal change of the Mindanao Current: Is there a robust trend?. *Geophysical Research Letters*, *46*, 6755–6764. https://doi.org/10.1029/2019GL083090

Received 30 MAR 2019
Accepted 28 MAY 2019
Accepted article online 5 JUN 2019
Published online 24 JUN 2019

Multidecadal Change of the Mindanao Current: Is There a Robust Trend?

Jing Duan[1,2,3], Yuanlong Li[1,2,3], Fan Wang[1,2,3], and Zhaohui Chen[3,4]

[1]CAS Key Laboratory of Ocean Circulation and Waves, Institute of Oceanology, Chinese Academy of Sciences, Qingdao, China, [2]Center for Ocean Mega-Science, Chinese Academy of Sciences, Qingdao, China, [3]Function Laboratory for Ocean Dynamics and Climate, Qingdao National Laboratory for Marine Science and Technology, Qingdao, China, [4]Physical Oceanography Laboratory, Ocean University of China, Qingdao, China

Abstract Ten ocean state estimate products are analyzed to quantify the multidecadal change of the Mindanao Current (MC). These data sets suggest multidecadal trends of the MC transport since 1961, 1980, and 1993 are weak (-0.3 Sv, +0.7 Sv, and +2.1 Sv, respectively; 1 Sv ≡ 10^6 m^3/s) and not robust with respect to the large spread of different data sets. The primary cause is the discrepancies in different wind data sets, and change of the North Equatorial Current's bifurcation latitude also acts to attenuate the MC change. The bifurcation latitude shifts southward (northward) under enhanced (weakened) northeasterly trade winds and feeds less (more) water to the MC. Experimental simulations of a reduced-gravity model forced by reanalysis and model-projected wind trends suggest an asymmetry of the MC's response to wind forcing. Anomalous westerly winds in the western Pacific can dramatically enhance the MC through spinning up the cyclonic local recirculation.

Plain Language Summary Here we attempt to estimate how much the Mindanao Current (MC) has changed over the past decades using 10 ocean state estimate products. The multidecadal trends of the MC volume transport since 1961, 1980, and 1993 were rather weak. We found large discrepancies in the MC's long-term change among different data sets, which are primarily due to uncertainties in surface wind data. The bifurcation point of the North Equatorial Current shifts to the south when the northeasterly trade winds are strengthened and shifts to the north under weakened northeasterly trade winds, which is a process attenuating the MC's change. Spatial structure of the surface wind trend over the Pacific basin is critical in determining the MC's long-term change. We performed simple model experiments and demonstrated that strong westerly wind trends in the western Pacific are particularly favorable for enhancing the MC. Under such condition, a strong cyclonic recirculation with strong mesoscale eddy activity emerges near the western boundary and enhances the MC in a nonlinear manner.

1. Introduction

The Mindanao Current (MC) originates from the bifurcation of trade wind-driven, westward-flowing North Equatorial Current (NEC) at ~13°N near the Philippines (e.g., Qiu & Lukas, 1996; Qu & Lukas, 2003; Toole et al., 1990). It flows southward along the Mindanao coast to ~4°N, feeding the Indonesian throughflow and the North Equatorial Countercurrent (NECC) with North Pacific water (e.g., Fine et al., 1994; Kashino et al., 2001; Li & Wang, 2012; Philander et al., 1987; Qu et al., 1999). The MC's variability in either volume transport or water temperature can be important for heat redistribution over the tropical Indo-Pacific Oceans (Hu et al., 2015; Lukas et al., 1996). The MC also serves as a route of the Pacific shallow meridional overturning circulation (McCreary & Lu, 1994), conveying subtropical variability signals to the equator and participating in the climate variabilities on decadal and longer time scales (e.g., Gu & Philander, 1997; Schneider, 2000; Zhang et al., 1998). Changes of the MC also affect the regional biological patterns and fishery over the western Pacific Ocean (e.g., Kimura et al., 2001; Lin et al., 2017).

As the western boundary current of the wind-driven North Pacific tropical gyre (Stommel, 1948), the MC's temporal variabilities on semiannual-to-decadal time scales were explained on the lowest order as the linear response to tropical trade wind forcing (e.g., Hu et al., 2016; Kim et al., 2004; Qiu & Chen, 2010; Qiu & Lukas, 1996; Ren et al., 2018). The dramatic changes in the tropical Pacific winds over the past decades (e.g., Meng

10.1029/2019GL083090

et al., 2012; Merrifield, 2011; Vecchi et al., 2006), of both natural and anthropogenic origins, may cause a significant multidecadal trend in the MC's strength. Existing studies have reported notable multidecadal trends of the western Pacific upper circulation, although such study for the MC is still lacking. Chen and Wu (2012) found that the NEC's bifurcation latitude (NBL), which determines water partition between the MC and the Kuroshio Current (KC), migrated equatorward from 15.5°N to 13.9°N over 1950-2008. Based on 12 ocean reanalysis products, Hsin (2016) suggested that the NEC in the western Pacific was slowly strengthening (+0.016 Sv/year; 1 Sv ≡ 10^6 m^3/s) from 1960s to 2000s. Using satellite altimeter data since 1993, the NEC, NECC, and KC were suggested to be strengthening (Qiu & Chen, 2012; Wu et al., 2016). Observational data and model simulations suggested a dramatic enhancement of the Indonesian throughflow since the 1980s (e.g., Feng et al., 2016; Lee et al., 2015; Liu et al., 2015; Sprintall et al., 2014) owing to the negative phase of the Interdecadal Pacific Oscillation (IPO; e.g., Power et al., 1999; England et al., 2014). Since the MC is connected with these currents, a robust multidecadal trend of this important current is likely. In a recent paper, Duan et al. (2019) documented prominent decadal variations of the MC, in which the linear trend was not studied.

Quantifying and examining the multidecadal change of the MC during the past half century are helpful for understanding the response of the ocean circulation to climate change. Here this is pursued by analyzing 10 long-term ocean state estimates (OSEs) based on model simulations and reanalysis systems. Our results reveal large discrepancies among these state-of-the-art OSE products and very weak/insignificant ensemble trend of the MC transport. Simplified ocean model experiments are performed to understand the underlying causes and examine the sensitivity of the MC trend to wind forcing characteristics.

2. Data and Methods

We analyzed 10 monthly OSE data sets covering 1961–2010. While Oceanic General Circulation Model for the Earth Simulator (OFES) is an eddy-resolving (0.1° × 0.1°) ocean model simulation without data assimilation, the other nine are ocean/climate model reanalysis products with horizontal resolutions ranging from 0.25° to 1.4°. Detailed information of them is summarized in Table S1 in the supporting information. The 10 OSEs are forced/coupled with 10 different wind data sets, which are also analyzed here. Moreover, wind stress data from future projection (2006-2100) of Representative Concentration Pathways 8.5 scenario from 25 Coupled Model Intercomparison Project Phase 5 (CMIP5) models (Table S2) are also analyzed.

To validate OSEs, sea surface height and surface geostrophic current from Archiving Validation and Interpretation of Satellite Oceanography (AVISO) and sea level records of two tidal gauge stations located near the Mindanao coast (Davao at 7.83°N, 125.63°E; Malakal at 7.33°N, 134.45°E) are used. Most of the OSEs agree well with AVISO data in climatological locations and structures of the western Pacific circulation (Figures S1a–S1k). Six of the OSEs provide sea surface height data, which agree well with AVISO in the Mindanao Dome (MD) region (127–160°E, 2–10°N) and consistent with the two tide gauge records over 1969-2010 (Figure S1).

The volume transport of the MC is computed by integrating southward velocity over 0-500 m at 8°N from the Mindanao coast to 130°E (Figure S1k). Similarly, the NEC transport at 130°E is the integration of 0- to 500-m westward velocity between 8°N and 18°N, while the KC transport is that of northward velocity at 18°N from the Luzon coast to 130°E. The NBL is defined as the latitude where the 0- to 500-m meridional transport within 2° band off the Philippine coast equals zero (Chen & Wu, 2011, 2012; Qiu & Lukas, 1996). Ekman pumping velocity is calculated as $w_E = curl(\tau/f)\rho^{-1}$, where τ is the wind stress vector and $\rho = 1{,}025$ kg/m^3 is sea water density. For all the variables mentioned above, the monthly climatology is removed, and the linear trend is estimated using a least squares fitting and presented in results in the form of total change over the target period.

To elucidate wind forcing effect, a 1.5-layer nonlinear reduced-gravity ocean (RGO) model is used. This model is configured to the Pacific Ocean basin between 100°E-70°W and 20°S-40°N with horizontal resolutions of 0.25° × 0.25°. For model equations and parameterizations, readers can refer to Chen and Wu (2011) and Duan et al. (2019). After a spin-up of 20 years under climatological wind forcing, 10 model runs are performed, forced by 10 wind data sets of OSEs for the period of 1961-2010.

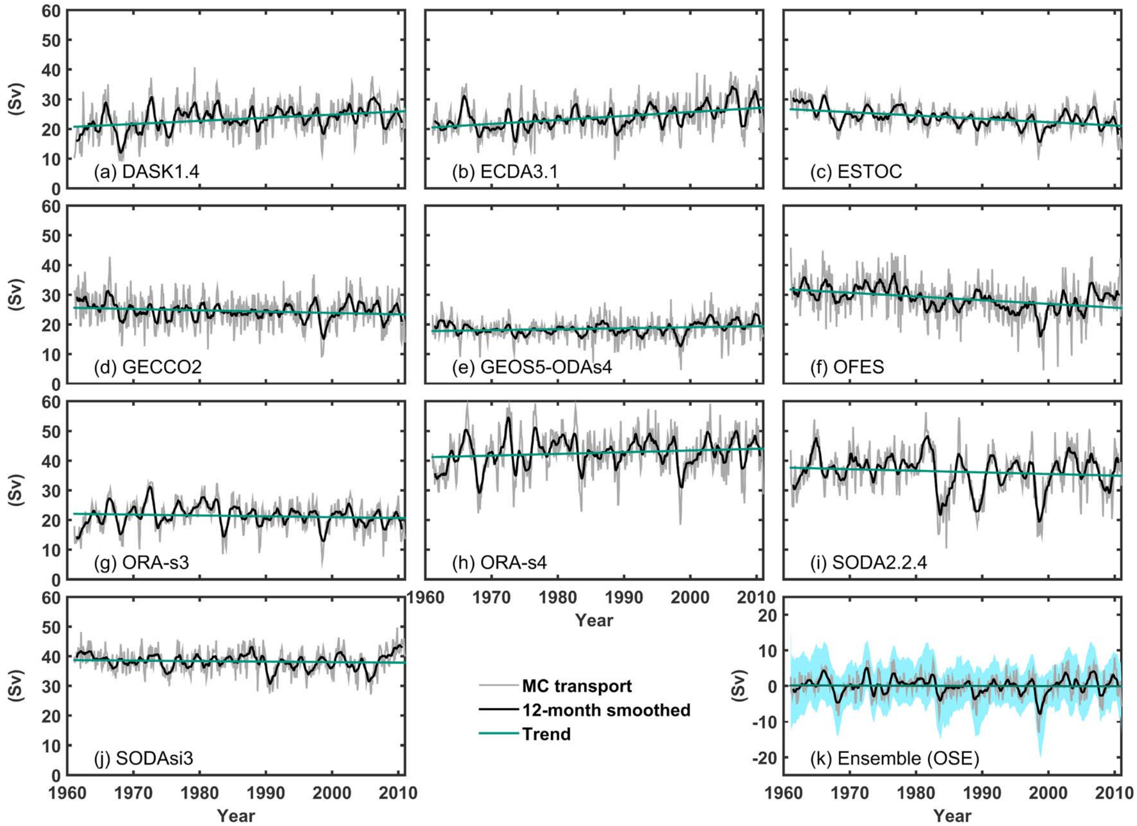

Figure 1. Monthly Mindanao Current volume transport (gray) at 8°N derived from (a) DASK1.4, (b) ECDA3.1, (c) ESTOC, (d) GECCO2, (e) GEOS5-ODAs4, (f) OFES, (g) ORA-s3, (h) ORA-s4, (i) SODA2.2.4, (j) SODAsi3, and (k) ensemble mean of their anomalies. Black curve denotes the 12-month smoothed Mindanao Current transport, and green line denotes the linear trend of 1961-2010. Blue shading in (k) shows the standard deviation of 10 ocean state estimates (OSEs).

3. Results: Multidecadal Trend of the MC

The period 1961-2010 is the longest for which the 10 OSEs are all available. This period may be suitable for examining the MC's response to anthropogenic climate change, since the IPO was generally situated in its negative phase during both the 1960s and 2000s. Volume transport of the MC at 8°N shows strong interannual variations of 10-20 Sv in all the 10 OSEs (Figure 1). Most of the products do not exhibit evident linear trends over the entire period. Only Estimated State of Ocean for Climate Research version 03a (ESTOC) and OFES show significant weakening trends, and Data Assimilation System of Korea Institute of Ocean Science and Technology version 1.4 (DASK1.4) and Geophysical Fluid Dynamics Laboratory Ensemble Coupled Data Assimilation Experiment version 3.1 (ECDA3.1) show strengthening trends. Note that both ESTOC and OFES are forced by National Centers for Environmental Prediction/National Center for Atmospheric Research (NCEP-NCAR) winds, although ESTOC system corrects surface air-sea fluxes through data assimilation. The MC trend is likely sensitive to the choice of wind data. The multiproduct ensemble mean (MEM) MC (Figure 1k) shows very weak trend (-0.3 Sv over 1961-2010), which is far from significant. Given the prominent interproduct discrepancies, the MC's trend for 1961-2010 is not robust.

Observational data were quite sparse for both ocean and atmosphere before 1980, causing difficulties for ocean models/reanalysis systems to realistically represent oceanic change. We therefore also examine the trends since 1980 and 1993. Wind data have been more reliable since 1980 due to the advent of atmosphere satellite observations. Satellite altimeter data have been available for ocean assimilation since 1993, greatly strengthening the fidelity of reanalysis products. During the 1980s to 1990s, the IPO was generally positive with strong and frequent El Niño events and weak trade winds and gradually shifted to the negative phase of the 2000s with strengthened trade winds (England et al., 2014). Therefore, the MC changes during these two periods mainly reflect the IPO effect. The MC transport in MEM was increased by +2.1 Sv during 1993-2010 (Figure 2a). ECDA3.1, Goddard Earth Observing System Model integrated Ocean Data Assimilation System

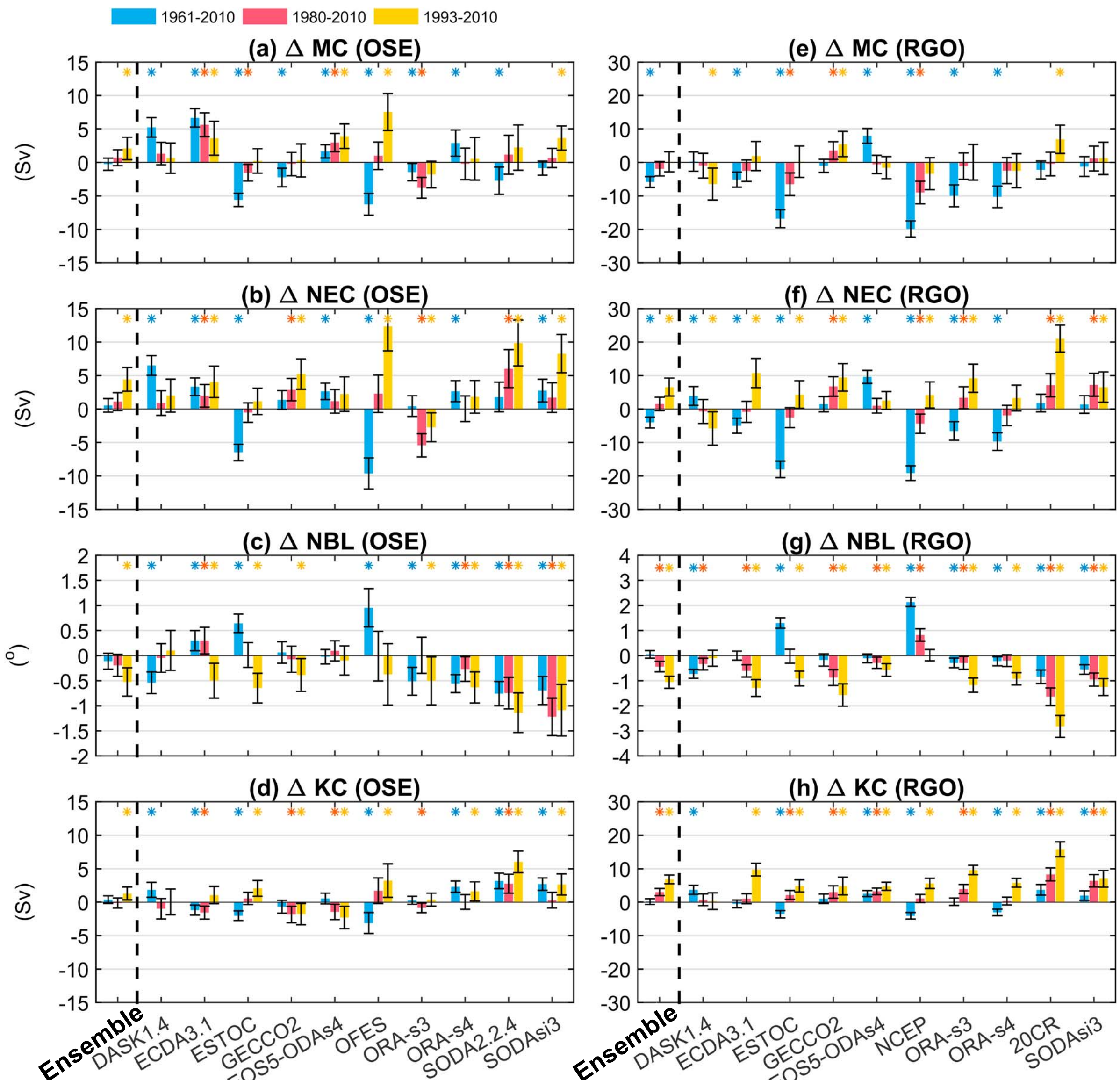

Figure 2. Linear trends of the (a) Mindanao Current (MC), (b) North Equatorial Current (NEC), (c) NEC's bifurcation latitude (NBL), and (d) Kuroshio Current (KC) for the periods of 1961-2010, 1980-2010, and 1993-2010 derived from 10 ocean state estimates (OSEs). Error bars indicate the 95% confidence interval, and asterisks denote exceeding 95% significance. (e–h) Same as (a–d) but from reduced-gravity ocean (RGO) model runs.

version 4 (GEOS5-ODAs4), OFES, and Simple Ocean Data Assimilation with sparse observational input version 3 (SODAsi3) are the primary contributors, with no significant trends in the other six OSEs. This trend is weak compared with its interannual variability of O(10 Sv) and mean value of 28.3 Sv based on MEM.

Strengthening of the MC was linked to that of the NEC (+4.2 Sv in MEM; Figure 2b), as the response to the enhanced northeasterly trade winds during this period. The transport increase of the MC is only one half of that of the NEC. This is due to the southward shift of the NBL. In MEM, the NBL trend is -0.53° over 1993-2010, and 7 out of 10 OSEs show significant southward migrations (Figure 2c). More water of the NEC joined the KC (Figure 2d), and the MC increase was attenuated. Note that the +2.1 Sv trend of the MC for 1993-2010 is marginally significant, with an error bar close to the trend value, and no longer significant if OFES is removed. We therefore conclude that the MC's trend from 1993 to 2010 is also not robust. The case of 1980-2010 is similar, with no significant trends of the MC, NEC, and NBL and evident discrepancies of different data sets.

10.1029/2019GL083090

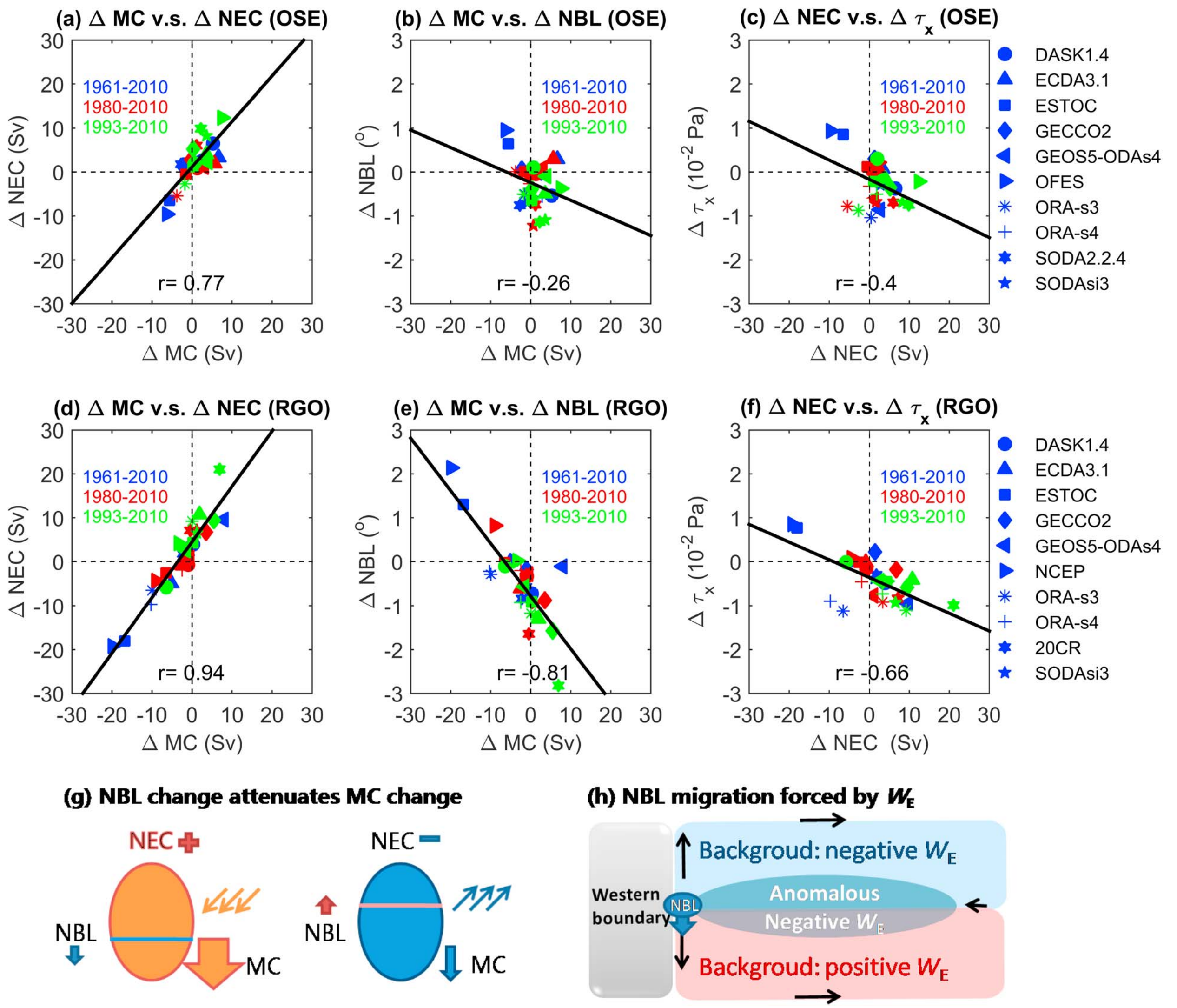

Figure 3. Scatterplots of (a) Mindanao Current (MC) versus North Equatorial Current (NEC), (b) MC versus NEC's bifurcation latitude (NBL) and (c) NEC versus zonal wind stress τ_x of 8–18°N, 120°E-70°W in temporal change for the periods of 1961-2010, 1980-2010, and 1993-2010 derived from 10 ocean state estimates (OSEs). (d–f) Same as (a)–(c) but from reduced-gravity ocean (RGO) model runs. Schematic of (g) damping effect of the NBL change on the MC change and (h) the influence of the anomalous w_E on the migration of the NBL.

The above analysis of OSEs overall suggests very weak and insignificant multidecadal MC changes and widespread of different data sets. Similar results are obtained by simulations of a 1.5-layer RGO model forced with the OSE's wind stress fields (Figures 2e–2h). Comparisons of OSEs and RGO model runs (hereafter RGOs) in the trends of MC, NEC, KC, and NBL are shown in Figure S2. The significant correlations between OSEs and RGOs ($r \geq 0.4$) confirm the importance of wind forcing determining the MC trend, since in the 1.5-layer RGO model oceanic variability is mainly caused by wind stress changes through first-mode baroclinic response. For the 1961-2010 period, RGOs produce significant reductions of the MC and NEC (-5.8 and -4.0 Sv in MEM, respectively; Figures 2e and 2f), particularly under winds of ECDA3.1, ESTOC, NCEP-NCAR, European Centre for Medium-Range Weather Forecasts Ocean Reanalysis System 3 (ORA-s3), and European Centre for Medium-Range Weather Forecasts Ocean Reanalysis System 4 (ORA-s4). For 1993-2010, the RGOs suggest an increase of the NEC by +6.5 Sv, stronger than that in OSEs. However, the MC does not show evident enhancement during this period, owing to the NBL's southward migration of 1.1°. Discrepancies between RGOs and OSEs may arise from various sources, such as data assimilation in OSEs and missed processes in the RGO model such as higher-order modes and buoyancy flux effect. Nevertheless, the OSEs and RGOs reach consensus in voting down a robust trend of the MC. Below we explore the possible causes.

Both OSEs and RGOs suggest that the NBL change can attenuate the MC change stemmed from the NEC and is partly responsible for the weak MC trends. Figures 3a and 3d demonstrate that the MC change and the NEC change bear a tight relationship (r = 0.77 for OSEs and r = 0.94 for RGOs). The NBL change, by contrast, shows a negative correlation with the MC change (r = -0.26 for OSEs and r = -0.81 for RGOs; Figures 3b and 3e). Note that the negative correlation in OSEs is largely contributed by ESTOC and OFES and vanishes if they are removed. Therefore, here we mainly explain the NBL's damping effect on the MC change in RGO results. The NBL generally shifts southward (northward), which reduces (raises) the water partition of the NEC to the MC and attenuates the MC change caused by the NEC. This exerts a damping effect on the MC's trend. During 1993-2010, the KC is strengthened by +1.3 Sv in OSEs and +6.8 Sv in RGOs (Figures 2d and 2h) as the result of the strengthened NEC and the southward shift of the NBL. The KC change shows a negative correlation with the NBL change (-0.76 and -0.84; Figures S3b and S3e), confirming this relationship. Therefore, in sharp contrast to the case of the MC, the KC's trend is strengthened by the NBL shift.

The negative correlation between the NEC change and the NBL change (Figures S3c and S3f) is critical (r = -0.62 in OSEs and r = -0.88 in RGOs), which implies that the NBL shifts southward (northward) when the NEC is strengthened (weakened) and generally acts to attenuate the MC change (see Figure 3g for the schematic). This negative correlation can be understood by considering the spatial structure of surface winds. The total transport of the NEC is largely determined by the strength of the Pacific trade winds, as indicated by the negative correlation (Figures 3c and 3f) between the NEC change and zonal wind stress τ_x change. The northeasterly trade winds in the North Pacific are accompanied with negative w_E (or negative wind stress curl) north of 10°N (Figures S4a and S4b). Strengthening of the trade winds also enhances the negative w_E at the NBL latitudes and drives a southward migration of the NBL (see Figure 3h for the schematic; e.g., Qiu & Chen, 2010; Chen & Wu, 2012).

4. Discussion: Sensitivity to Wind Forcing Characteristics

Although the NBL change can suppress the MC change, characteristics of surface wind trend are deterministic for the MC's multidecadal trend. Given the wide spread of wind data sets, it is unknown which one is more reliable. For the 1961-2010 period, the NCEP-NCAR and ESTOC winds favor a significant weakening of the MC (Figures 2a and 2e), because of the weakening trade winds in these two data sets (Figures 3c and 3f). This means that the MC can show strong multidecadal trend if suitable wind forcing is exerted. In this section we examine the sensitivity of the MC to surface wind trend characteristics. In other words, we answer the question as to what type of wind trend (direction, spatial pattern, and strength) is the most favorable in generating strong trend of the MC. To do so, we conduct two groups of experimental RGO model runs, for which the wind forcing is expressed as $\boldsymbol{\tau} = \boldsymbol{\tau}_{clim} + R \times \boldsymbol{\tau}_{\mathrm{trend}}$, where $\boldsymbol{\tau}_{clim}$ and $\boldsymbol{\tau}_{\mathrm{trend}}$ are the monthly climatology and linear trend of wind stress and R is the ratio ranging from -300% to +300% with intervals of 20%. The $\boldsymbol{\tau}_{clim}$ adopts the average of selected six products (ESTOC, GECCO2, NCEP-NCAR, ORA-s3, ORA-s4, and SODAsi3), which have more realistic climatological w_E distribution. The other four products cannot correctly represent the positive basin-mean w_E at the latitudes of the MC and are therefore discarded (Figures not shown).

For the first group, $\boldsymbol{\tau}_{\mathrm{trend}}$ is the ensemble mean trend of the six products for 1961-2010 (Figures S4c and S4d). The trend structure largely resembles the central Pacific-type La Niña (e.g., Shinoda et al., 2011), showing evident divergence of surface winds in the central Pacific (Figure S4c). The western (eastern) Pacific Ocean is controlled by easterly (westerly) wind and negative (positive) off-equatorial w_E trends. Recent researches suggested that the quicker warming of the Indian and Atlantic Oceans than the Pacific under greenhouse gas forcing may be responsible for this wind trend pattern (e.g., Han et al., 2014; Luo et al., 2012; McGregor et al., 2014). For the second group, $\boldsymbol{\tau}_{\mathrm{trend}}$ is the ensemble-mean-projected wind stress trend of 25 CMIP5 models for 2006-2100 in Representative Concentration Pathways 8.5 scenario (hereafter the CMIP5 projection wind). CMIP5 models project a basin-wide weakening of the trade winds over the equatorial and tropical North Pacific regions (5°S-25°N; Figures S4e and S4f) corresponding to the projected El Niño-like surface warming pattern (Sen Gupta et al., 2012; Vecchi & Soden, 2007; Xie et al., 2010). All the experiments are integrated for 50 years, and the last 5 years are analyzed (Figure 4). The deviation of one experiment from the $R = 0$ experiment represents its trend.

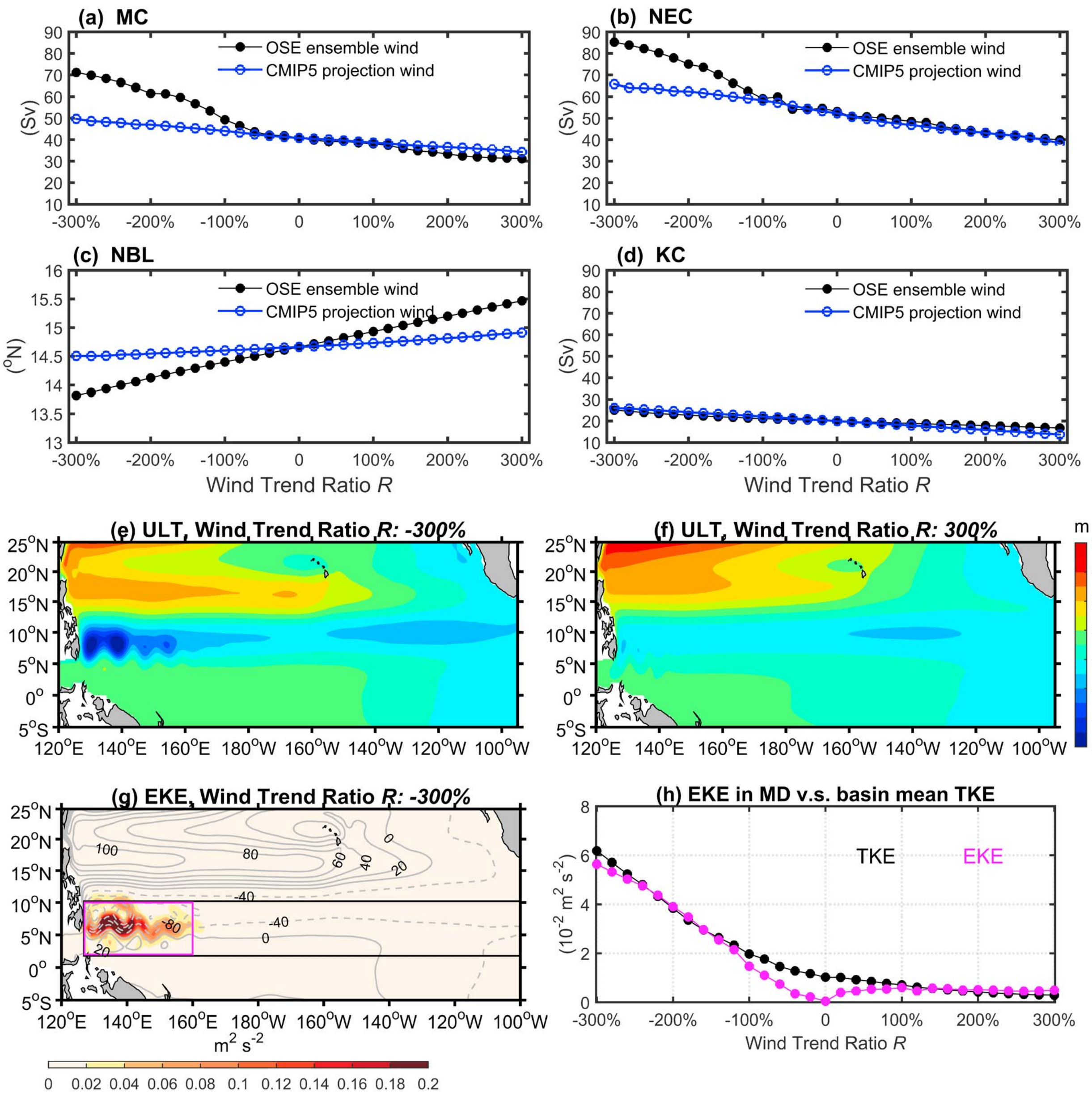

Figure 4. The (a) Mindanao Current (MC), (b) North Equatorial Current (NEC), (c) NEC's bifurcation latitude (NBL), and (d) Kuroshio Current (KC) of the last 5 years of the experimental reduced-gravity ocean model runs forced by ocean state estimate (OSE) wind trend and Coupled Model Intercomparison Project Phase 5 (CMIP5) projection wind trend as functions of R ranging from -300% to +300%. Upper layer thickness (ULT) of the last 5 years of the OSE wind-forced RGO model runs for (e) R = -300% and (f) R = +300%. (g) Same as (e) but for eddy kinetic energy (EKE), and contours denote the mean ULT. (h) Average EKE of the Mindanao Dome and basin-mean total kinetic energy (TKE) of the tropical gyre (areas are shown as pink and black boxes in Figure 4g) of the OSE wind-forced reduced-gravity ocean model runs, as functions of R.

The response of the MC to CMIP5 projection winds is in a linear manner, showing nearly symmetric changes for positive and negative ratios. The MC is weakened by -2.2 Sv at +100% wind trend, and under +300% wind trend, the MC change is -6.6 Sv. The responses of the NEC, NBL, and KC to the projected wind trends are also linear. Under weakened trade winds, the NBL shifts northward to partly offset the MC weakening, and the KC transport is also reduced (e.g., Duan et al., 2017). Therefore, zonally uniform, weak trends of the Pacific trade winds as in CMIP5 model projection generally induce linear response of the Philippine Sea circulation, and the MC's trend tends to be weak. By contrast, OSE ensemble wind trend induces asymmetric responses of the NEC and the MC. When R increases from 0% to 300%, their changes are quasi-linear, but when R decreases from 0% to -300%, the MC and the NEC are enhanced in a nonlinear manner. The nonlinearity emerges around R = -60%. When R = -100% (opposite to Figure S4c), the MC is enhanced by +8.5 Sv, equivalent to that at R = -300% under CMIP5 projection winds. At R = -300%, the MC transport is increased to as large as 71.1 Sv and enhanced by more than 70%. This means that strong westerly wind trends/anomalies in the western Pacific switch on the nonlinearity of the Philippine Sea circulation system. It is interesting to note that this nonlinearity resides merely in the NEC and MC, not in the NBL and KC.

Here we propose the possible nonlinear process affecting the MC change. The MD is the cyclonic recirculation with shoaled thermocline in the far western Pacific (e.g., Kashino et al., 2011; Masumoto & Yamagata, 1991). The strength of the MD is tied through geostrophy with transports of the MC, NEC, and NECC. In OSE wind-forced RGO model runs, the MD can be quantified by negative change of upper layer thickness values. It is much stronger at R = -300% than at R = +300% (Figures 4e and 4f), with a train of mesoscale cyclonic recirculation structures. The eddy kinetic energy (EKE) computed with upper-layer current anomaly also shows high values within the MD region at R = -300% (Figure 4g). Figure S5 suggests that high EKE values appear in the MD region since R = -60%, which is roughly the point at which the nonlinear growth of the MC begins. The maximal EKE value locates on the northern flank of the NECC where mesoscale eddies are active (Chen et al., 2015; Zhao et al., 2013). The nonlinear growth of the MC strength with decreasing R is probably associated with these eddy-like recirculation structures.

Figure 4h suggests roughly consistent change of the EKE in the MD region and the total kinetic energy (TKE) of the entire tropical gyre. Both EKE and TKE are prevailingly low for R = -60% ~ +300%, and for R < -60% the two show abrupt increase. The resemblance of EKE and TKE indicates that the eddy-like local recirculation (quantified by EKE) gains energy from the enhanced large-scale circulation (quantified by TKE). As such, the positive relative vorticity anomalies input by the westerly wind anomalies in the western-central Pacific basin tend to concentrate near the western boundary, which greatly enhances the MC and NEC in the Philippine Sea.

The above results suggest that regionally enhanced westerly wind anomalies in the western Pacific Ocean are most favorable for producing strong strengthening trend of the MC and the MC shows asymmetric response to westerly and easterly anomalies. These results complement to the existing linear mechanisms of the Philippine Sea circulation variability. Westerly winds in the western Pacific are required to sufficiently spin up the tropical gyre and invoke nonlinear growth of local recirculation. This situation is similar to westerly wind bursts during El Niño events (e.g., Menkes et al., 2014), and dramatic strengthening of the MD and NEC has been observed (Kashino et al., 2009; Zhao et al., 2013). Investigation of the nonlinear processes with more complicated models is required to achieve more in-depth understanding, which is our ongoing research.

5. Summary

Variability of the MC is important of heat redistribution over the tropical Indo-Pacific Oceans. In this study, multidecadal change of the MC is quantified by analyzing 10 OSEs, and causes are investigated with a 1.5-layer RGO model. The MC in MEM shows weak and insignificant trends since 1961, 1980, and 1993. We also examined the MC trends at 7°N and 9°N, and the similar results are achieved (figures not shown). The 10 OSEs show large spread in the MC's long-term trend, which is mainly attributed to the evident discrepancies in wind data sets. The NBL change acts to attenuate the MC change. It shifts southward (northward) under enhanced (weakened) northeasterly trade winds, feeding less (more) NEC water to the MC.

Experimental runs of the RGO model with various wind forcing fields suggest a nonlinear behavior of the MC transport. Regionally enhanced westerly wind trends in the western Pacific are particularly favorable for enhancing the MC, through invoking the nonlinear growth of the local recirculation structures. When the tropical gyre is sufficiently spun up by westerly winds, kinetic energy is transferred to the cyclonic recirculation probably through dynamical instability. As such, the positive relative vorticity anomalies derived from winds tend to enhance the MD, and the MC is greatly enhanced. Our results highlight the necessity of exploring the nonlinear processes to promote our understanding of regional ocean dynamics.

Acknowledgments
The authors thank two anonymous reviewers for providing insight comments. This study is supported by the National Natural Science Foundation of China (NSFC; Grants 41806014, 41730534, 41776001, 41806001, and 41622602) and the AoShan Talents Program (2017ASTCP-ES05). AVISO data are downloaded online (from http://www.aviso.oceanobs.com/). Tidal gauges data are available online (at https://www.psmsl.org/). Availability of the 10 OSEs is described in Table S1. 20CR v2 winds and NCEP-NCAR winds are both obtained from NOAA's PSD website (https://www.esrl.noaa.gov/psd/data/gridded/). CMIP5 model wind data sets can be downloaded online (at http://cmip-pcmdi.llnl.gov/cmip5/).

References

Chen, L., Jia, Y., & Liu, Q. (2015). Mesoscale eddies in the Mindanao Dome region. *Journal of Oceanography*, *71*(1), 133–140. https://doi.org/10.1007/s10872-014-0255-3

Chen, Z., & Wu, L. (2011). Dynamics of the seasonal variation of the North Equatorial Current bifurcation. *Journal of Geophysical Research*, *116*, C02018. https://doi.org/10.1029/2010JC006664
Chen, Z., & Wu, L. (2012). Long-term change of the Pacific North Equatorial Current bifurcation in SODA. *Journal of Geophysical Research*, *117*, C06016. https://doi.org/10.1029/2011JC007814
Duan, J., Chen, Z., & Wu, L. (2017). Projected changes of the low-latitude north-western Pacific wind-driven circulation under global warming. *Geophysical Research Letters*, *44*, 4976–4984. https://doi.org/10.1002/2017GL073355
Duan, J., Li, Y., Wang, F., & Chen, Z. (2019). Decadal variations of the Mindanao Current during 1960-2010. *Journal of Geophysical Research: Oceans*, *124*, 2660–2678. https://doi.org/10.1029/2019JC014975
England, M. H., McGregor, S., Spence, P., Meehl, G. A., Timmermann, A., Cai, W., et al. (2014). Recent intensification of wind-driven circulation in the Pacific and the ongoing warming hiatus. *Nature Climate Change*, *4*(3), 222–227. https://doi.org/10.1038/nclimate2106
Feng, M., Zhang, X., Oke, P., Monselesan, D., Chamberlain, M., Matear, R., & Schiller, A. (2016). Invigorating ocean boundary current systems around Australia during 1979-2014: As simulated in a near-global eddy-resolving ocean model. *Journal of Geophysical Research: Oceans*, *121*, 3395–3408. https://doi.org/10.1002/2016JC011842
Fine, R. A., Lukas, R., Bingham, F. M., Warner, M. J., & Gammon, R. H. (1994). The western equatorial Pacific: A water mass crossroads. *Journal of Geophysical Research*, *99*(C12), 25063. https://doi.org/10.1029/94JC02277
Gu, D., & Philander, S. G. H. (1997). Interdecadal climate fluctuations that depend on exchanges between the tropics and extratropics. *Science*, *275*(5301), 805–807. https://doi.org/10.1126/science.275.5301.805
Han, W., Meehl, G. A., Hu, A., Alexander, M. A., Yamagata, T., Yuan, D., et al. (2014). Intensification of decadal and multi-decadal sea level variability in the western tropical Pacific during recent decades. *Climate Dynamics*, *43*(5–6), 1357–1379. https://doi.org/10.1007/s00382-013-1951-1
Hsin, Y.-C. (2016). Trends of the pathways and intensities of surface equatorial current system in the North Pacific Ocean. *Journal of Climate*, *29*(18), 6693–6710. https://doi.org/10.1175/JCLI-D-15-0850.1
Hu, D., Wu, L., Cai, W., Gupta, A. S., Ganachaud, A., Qiu, B., et al. (2015). Pacific western boundary currents and their roles in climate. *Nature*, *522*(7556), 299–308. https://doi.org/10.1038/nature14504
Hu, S., Hu, D., Guan, C., Wang, F., Zhang, L., Wang, F., & Wang, Q. (2016). Interannual variability of the Mindanao Current/Undercurrent in direct observations and numerical simulations. *Journal of Physical Oceanography*, *46*(2), 483–499. https://doi.org/10.1175/JPO-D-15-0092.1
Kashino, Y., España, N., Syamsudin, F., Richards, K. J., Jensen, T., Dutrieux, P., & Ishida, A. (2009). Observations of the North Equatorial Current, Mindanao Current, and Kuroshio current system during the 2006/07 El Niño and 2007/08 La Niña. *Journal of Oceanography*, *65*(3), 325–333. https://doi.org/10.1007/s10872-009-0030-z
Kashino, Y., Firing, E., Hacker, P., Sulaiman, A., & Lukiyanto (2001). Currents in the Celebes and Maluku Seas, February 1999. *Geophysical Research Letters*, *28*(7), 1263–1266. https://doi.org/10.1029/2000GL011630
Kashino, Y., Ishida, A., & Hosoda, S. (2011). Observed ocean variability in the Mindanao Dome region. *Journal of Physical Oceanography*, *41*(2), 287–302. https://doi.org/10.1175/2010JPO4329.1
Kim, Y. Y., Qu, T., Jensen, T., Miyama, T., Mitsudera, H., Kang, H. W., & Ishida, A. (2004). Seasonal and interannual variations of the North Equatorial Current bifurcation in a high-resolution OGCM. *Journal of Geophysical Research*, *109*, C03040. https://doi.org/10.1029/2003JC002013
Kimura, S., Inoue, T., & Sugimoto, T. (2001). Fluctuation in the distribution of low-salinity water in the North Equatorial Current and its effect on the larval transport of the Japanese eel. *Fisheries Oceanography*, *10*(1), 51–60. https://doi.org/10.1046/j.1365-2419.2001.00159.x
Lee, S.-K., Park, W., Baringer, M. O., Gordon, A. L., Huber, B., & Liu, Y. (2015). Pacific origin of the abrupt increase in Indian Ocean heat content during the warming hiatus. *Nature Geoscience*, *8*(6), 445–449. https://doi.org/10.1038/ngeo2438
Li, Y., & Wang, F. (2012). Spreading and salinity change of North Pacific Tropical Water in the Philippine Sea. *Journal of Oceanography*, *68*(3), 439–452. https://doi.org/10.1007/s10872-012-0110-3
Lin, Y.-F., Wu, C.-R., & Han, Y.-S. (2017). A combination mode of climate variability responsible for extremely poor recruitment of the Japanese eel (Anguilla japonica). *Scientific Reports*, *7*(1), 44469. https://doi.org/10.1038/srep44469
Liu, Q.-Y., Feng, M., Wang, D., & Wijffels, S. (2015). Interannual variability of the Indonesian Throughflow transport: A revisit based on 30 year expendable bathythermograph data. *Journal of Geophysical Research: Oceans*, *120*, 8270–8282. https://doi.org/10.1002/2015JC011351
Lukas, R., Yamagata, T., & McCreary, J. P. (1996). Pacific low-latitude western boundary currents and the Indonesian throughflow. *Journal of Geophysical Research*, *101*(C5), 12209–12216. https://doi.org/10.1029/96JC01204
Luo, J.-J., Sasaki, W., & Masumoto, Y. (2012). Indian Ocean warming modulates Pacific climate change. *Proceedings of the National Academy of Sciences*, *109*(46), 18701–18706. https://doi.org/10.1073/pnas.1210239109
Masumoto, Y., & Yamagata, T. (1991). Response of the western tropical Pacific to the Asian winter monsoon: The generation of the Mindanao Dome. *Journal of Physical Oceanography*, *21*(9), 1386–1398. https://doi.org/10.1175/1520-0485(1991)021<1386:ROTWTP>2.0.CO;2
McCreary, J. P., & Lu, P. (1994). Interaction between the subtropical and equatorial ocean circulations: The subtropical cell. *Journal of Physical Oceanography*, *24*(2), 466–497. https://doi.org/10.1175/1520-0485(1994)024<0466:IBTSAE>2.0.CO;2
McGregor, S., Timmermann, A., Stuecker, M. F., England, M. H., Merrifield, M., Jin, F.-F., & Chikamoto, Y. (2014). Recent Walker circulation strengthening and Pacific cooling amplified by Atlantic warming. *Nature Climate Change*, *4*(10), 888–892. https://doi.org/10.1038/nclimate2330
Meng, Q., Latif, M., Park, W., Keenlyside, N. S., Semenov, V. A., & Martin, T. (2012). Twentieth century Walker Circulation change: Data analysis and model experiments. *Climate Dynamics*, *38*(9–10), 1757–1773. https://doi.org/10.1007/s00382-011-1047-8
Menkes, C. E., Lengaigne, M., Vialard, J., Puy, M., Marchesiello, P., Cravatte, S., & Cambon, G. (2014). About the role of Westerly Wind Events in the possible development of an El Niño in 2014. *Geophysical Research Letters*, *41*, 6476–6483. https://doi.org/10.1002/2014GL061186
Merrifield, M. A. (2011). A shift in western tropical Pacific sea level trends during the 1990s. *Journal of Climate*, *24*(15), 4126–4138. https://doi.org/10.1175/2011JCLI3932.1
Philander, S. G. H., Hurlin, W. J., & Seigel, A. D. (1987). Simulation of the seasonal cycle of the tropical Pacific Ocean. *Journal of Physical Oceanography*, *17*(11), 1986–2002. https://doi.org/10.1175/1520-0485(1987)017<1986:SOTSCO>2.0.CO;2
Power, S., Casey, T., Folland, C., Colman, A., & Mehta, V. (1999). Interdecadal modulation of the impact of ENSO on Australia. *Climate Dynamics*, *15*(5), 319–324. https://doi.org/10.1007/s003820050284

Qiu, B., & Chen, S. (2010). Interannual-to-decadal variability in the bifurcation of the North Equatorial Current off the Philippines. *Journal of Physical Oceanography*, *40*(11), 2525–2538. https://doi.org/10.1175/2010JPO4462.1

Qiu, B., & Chen, S. (2012). Multidecadal sea level and gyre circulation variability in the northwestern tropical Pacific Ocean. *Journal of Physical Oceanography*, *42*(1), 193–206. https://doi.org/10.1175/JPO-D-11-061.1

Qiu, B., & Lukas, R. (1996). Seasonal and interannual variability of the North Equatorial Current, the Mindanao Current, and the Kuroshio along the Pacific western boundary. *Journal of Geophysical Research*, *101*(C5), 12315–12330. https://doi.org/10.1029/95JC03204

Qu, T., & Lukas, R. (2003). The bifurcation of the North Equatorial Current in the Pacific*. *Journal of Physical Oceanography*, *33*(1), 5–18. https://doi.org/10.1175/1520-0485(2003)033<0005:TBOTNE>2.0.CO;2

Qu, T., Mitsudera, H., & Yamagata, T. (1999). A climatology of the circulation and water mass distribution near the Philippine Coast*. *Journal of Physical Oceanography*, *29*(7), 1488–1505. https://doi.org/10.1175/1520-0485(1999)029<1488:ACOTCA>2.0.CO;2

Ren, Q., Li, Y., Wang, F., Song, L., Liu, C., & Zhai, F. (2018). Seasonality of the Mindanao Current/Undercurrent System. *Journal of Geophysical Research: Oceans*, *123*, 1105–1122. https://doi.org/10.1002/2017JC013474

Schneider, N. (2000). A decadal spiciness mode in the tropics. *Geophysical Research Letters*, *27*(2), 257–260. https://doi.org/10.1029/1999GL002348

Sen Gupta, A., Ganachaud, A., McGregor, S., Brown, J. N., & Muir, L. (2012). Drivers of the projected changes to the Pacific Ocean equatorial circulation. *Geophysical Research Letters*, *39*, L09605. https://doi.org/10.1029/2012GL051447

Shinoda, T., Hurlburt, H. E., & Metzger, E. J. (2011). Anomalous tropical ocean circulation associated with La Niña Modoki. *Journal of Geophysical Research*, *116*, C12001. https://doi.org/10.1029/2011JC007304

Sprintall, J., Gordon, A. L., Koch-Larrouy, A., Lee, T., Potemra, J. T., Pujiana, K., & Wijffels, S. E. (2014). The Indonesian seas and their role in the coupled ocean–climate system. *Nature Geoscience*, *7*(7), 487–492. https://doi.org/10.1038/ngeo2188

Stommel, H. (1948). The westward intensification of wind-driven ocean currents. *Transactions, American Geophysical Union*, *29*(2), 202. https://doi.org/10.1029/TR029i002p00202

Toole, J. M., Millard, R. C., Wang, Z., & Pu, S. (1990). Observations of the Pacific North Equatorial Current bifurcation at the Philippine Coast. *Journal of Physical Oceanography*, *20*(2), 307–318. https://doi.org/10.1175/1520-0485(1990)020<0307:OOTPNE>2.0.CO;2

Vecchi, G. A., & Soden, B. J. (2007). Global warming and the weakening of the tropical circulation. *Journal of Climate*, *20*(17), 4316–4340. https://doi.org/10.1175/JCLI4258.1

Vecchi, G. A., Soden, B. J., Wittenberg, A. T., Held, I. M., Leetmaa, A., & Harrison, M. J. (2006). Weakening of tropical Pacific atmospheric circulation due to anthropogenic forcing. *Nature*, *441*(7089), 73–76. https://doi.org/10.1038/nature04744

Wu, C.-R., Wang, Y.-L., Lin, Y.-F., Chiang, T.-L., & Wu, C.-C. (2016). Weakening of the Kuroshio intrusion into the South China Sea under the global warming hiatus. *IEEE Journal of Selected Topics in Applied Earth Observations and Remote Sensing*, *9*(11), 5064–5070. https://doi.org/10.1109/JSTARS.2016.2574941

Xie, S.-P., Deser, C., Vecchi, G. A., Ma, J., Teng, H., & Wittenberg, A. T. (2010). Global warming pattern formation: Sea surface temperature and rainfall*. *Journal of Climate*, *23*(4), 966–986. https://doi.org/10.1175/2009JCLI3329.1

Zhang, R.-H., Rothstein, L. M., & Busalacchi, A. J. (1998). Origin of upper-ocean warming and El Niño change on decadal scales in the tropical Pacific Ocean. *Nature*, *391*(6670), 879–883. https://doi.org/10.1038/36081

Zhao, J., Li, Y., & Wang, F. (2013). Dynamical responses of the west Pacific North Equatorial Countercurrent (NECC) system to El Niño events. *Journal of Geophysical Research: Oceans*, *118*, 2828–2844. https://doi.org/10.1002/jgrc.20196